

# Hadron production and bottomonia suppression at the LHC

Georg Wolschin

Heidelberg University

Institut für Theoretische Physik

Philosophenweg 16

D-69120 Heidelberg

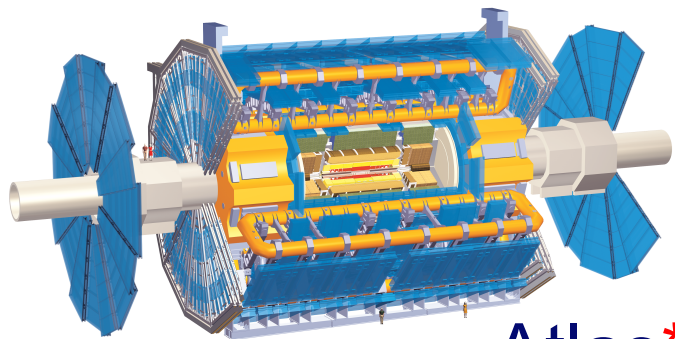


MESON 2014\_Krakow

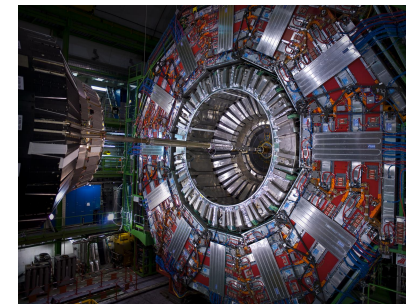
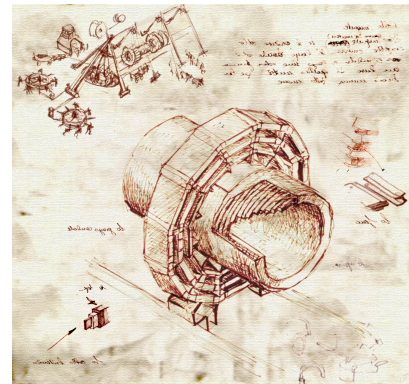
# Topics

1. Introduction: Relativistic heavy ions @ LHC; Stopping
2. Particle production: Relativistic Diffusion Model (RDM)
3. Bottomium suppression in the Quark-Gluon Plasma (QGP)
4. Conclusion

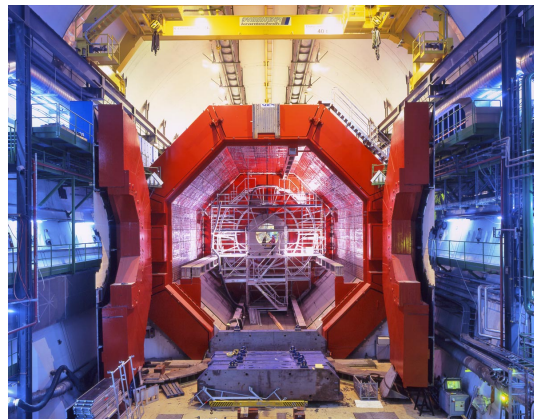
# 1. Introduction: LHC Detectors for Relativistic Heavy-Ion physics



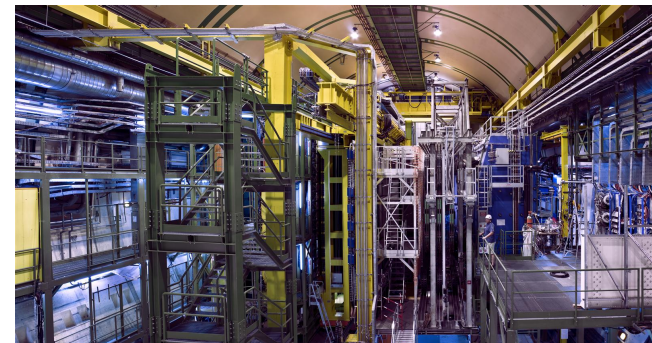
**Atlas\***  
≈ 25 HI people



**CMS\***  
da Vinci style  
≈ 60 HI people



**Alice\*:** L3 magnet  
≈ 1,000 HI people

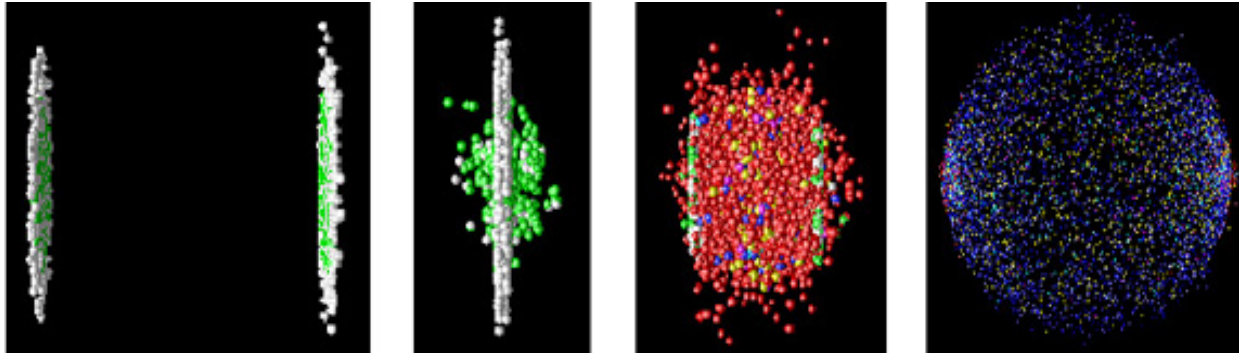


**LHCb**  
p-Pb only

\* heavy-ion capability

# Stopping: Net protons/baryons and gluon saturation

Stopping occurs mainly through the interaction of valence quarks with gluons

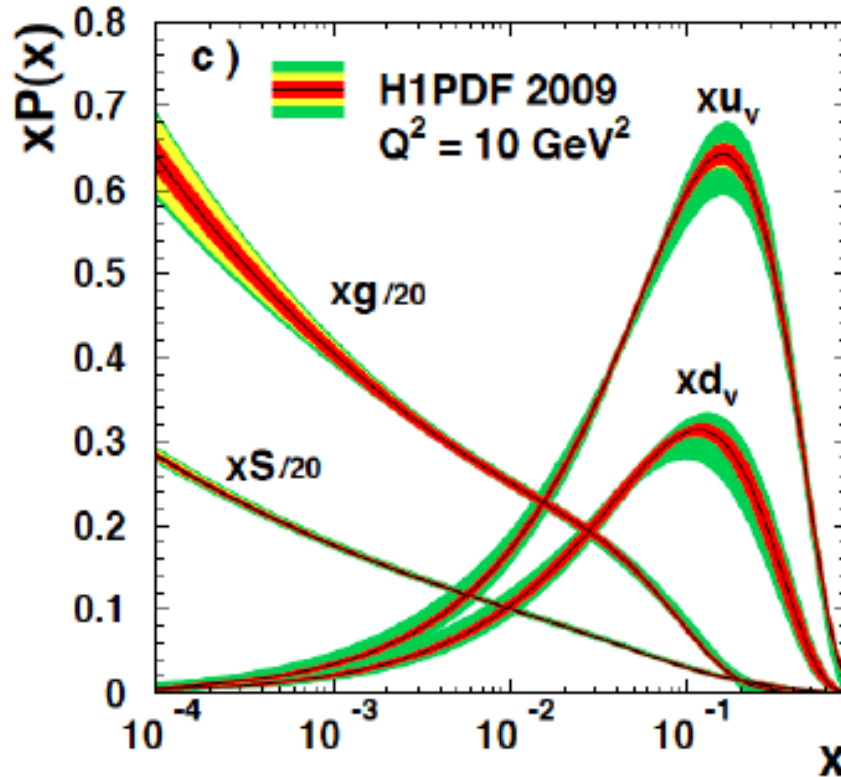


Artwork: UFRA

At RHIC ( $\leq 0.2$  TeV) and LHC ( $\leq 5.52$  TeV) energies, initially a state of very high gluon density is formed, which transforms into a strongly coupled quark-gluon plasma, and then hadronizes after  $\approx 10^{-23}$  s into mesons and baryons.

**Search for signatures of the QGP, and the initial Gluon Condensate in net-baryon (proton) distribution functions.**

QCD



Structure functions (pdfs)  
from e + p deep  
inelastic scattering (DIS)  
at HERA (DESY)

- ◆ Gluon structure functions grow with increasing  $Q^2$  and  $1/x$
- ◆ At **small x** and high energy, gluons dominate the dynamics.
- ◆ The gluon distribution should saturate at very small x. The saturation scale is

$$Q_s^2(x) \sim A^{1/3} x^{-\lambda}, \lambda \sim 0.3$$

→ Saturation effects should be more pronounced in nuclei

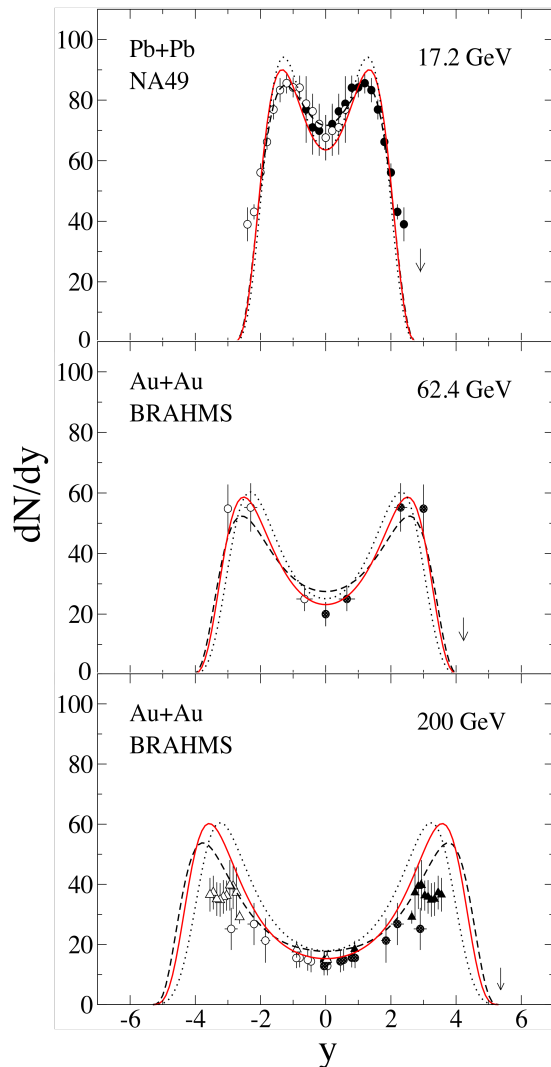
# Microscopic formulation of baryon transport for RHIC, LHC physics

- The net-baryon transport occurs through valence quarks:
- Fast valence quarks in one nucleus scatter in the other nucleus by exchanging soft gluons, and are redistributed in rapidity space.
- The valence quark parton distribution is well known at large  $x$ , which corresponds to the forward (and backward) rapidity region, and it can be used to access the small- $x$  gluon distribution in the target.

**Y. Mehtar-Tani and GW, Europhys. Lett. 94, 62003 (2011)**  
**Phys. Lett. B688, 174 (2010)**  
**Phys. Rev. C80, 054905 (2009)**  
**Phys. Rev. Lett. 102,182301 (2009)**

**GW, Prog. Part. Nucl. Phys. 59, 374 (2007)**  
**Phys. Rev. C 69, 024906 (2004)**

# Net-baryon rapidity distributions at SPS, RHIC, and LHC



➤ Central (0-5%) Pb+Pb (SPS) and Au+Au (RHIC) Collisions

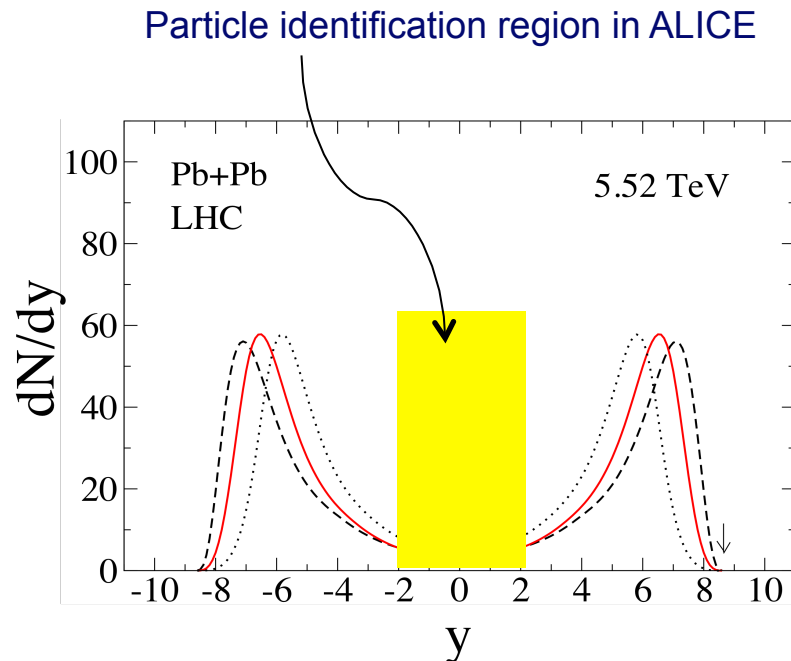
➤ Dashed black curves:  $Q_0^2 = 0.08 \text{ GeV}^2$ ,  $\lambda=0$   
 Solid red curves:  $Q_0^2 = 0.07 \text{ GeV}^2$ ,  $\lambda=0.15$   
 Dotted black curves:  $Q_0^2 = 0.06 \text{ GeV}^2$ ,  $\lambda=0.3$

➤ A larger gluon saturation scale produces more baryon stopping, as does a larger value of  $A$ .

➤ The saturation scale is  $Q_s^2(x) = A^{1/3} Q_0^2 x^{-\lambda}$

Y. Mehtar-Tani and GW, Phys. Rev. Lett. 102,182301 (2009).

# Net-baryon rapidity distributions at LHC: prediction



Y. Mehtar-Tani and GW  
Phys. Rev. Lett. 102,182301 (2009)

➤ Central (0-5%) Pb+Pb collisions,  $y_{beam} = 8.68$

➤ Dashed black curve:  $\lambda = 0$

Solid red curve:  $\lambda = 0.15$

Dotted black curve:  $\lambda = 0.3$

➤ **A larger gluon saturation scale produces more baryon stopping; the fragmentation peak position is sensitive to  $\lambda$**

➤ The midrapidity value of the net-baryon distribution is small, but finite:  
 $dN/dy (y = 0) \approx 4$ . The **total yield** is normalized to the number of baryon participants,  $N_B \approx 357$ .

**Measurements with particle identification will be confined to the yellow region for the next years**

## 2. Particle production: Relativistic Diffusion Model (RDM)

$$\frac{\partial}{\partial t} R(y, t) = -\frac{\partial}{\partial y} [J(y)R(y, t)] + D_y \frac{\partial^2}{\partial y^2} [R(y, t)]^{2-q}$$

R (y,t) Rapidity distribution function. The standard linear Fokker-Planck equation corresponds to  $q = 1$ , and a linear drift function. For the three components  $k = 1,2,3$  of the rapidity distribution,

$$\frac{\partial}{\partial t} R_k(y, t) = -\frac{1}{\tau_y} \frac{\partial}{\partial y} [(y_{eq} - y) \cdot R_k(y, t)] + D_y^k \frac{\partial^2}{\partial y^2} R_k(y, t)$$

Linear drift term with relaxation time  $\tau_y$       Diffusion term,  $D_y = \text{const.}$

Relaxation time and diffusion coefficient are related through a **dissipation-fluctuation theorem**. The broadening is enhanced due to collective expansion.

$$\langle y_{1,2}(t) \rangle = y_{eq} [1 - \exp(-t/\tau_y)] \mp y_{max} \exp(-t/\tau_y) \quad \text{mean value}$$

$$\sigma_{1,2,eq}^2(t) = D_y^{1,2,eq} \tau_y [1 - \exp(-2t/\tau_y)] \quad \text{variance}$$

**Linear Model:** G. Wolschin, Eur. Phys. J. A5, 85 (1999); with 3 sources: Phys. Lett. B 569, 67 (2003); PLB 698, 411 (2011); M. Biyajima, M. Ide, M. Kaneyama, T. Mizoguchi, and N. Suzuki, Prog. Theor. Phys. Suppl. 153, 344 (2004)

# Diffusion of produced particles in $\eta$ -space

Pseudorapidity distributions of produced particles are obtained through the Jacobian transformation

$$\frac{dN}{d\eta} = \frac{dN}{dy} \frac{dy}{d\eta} = \frac{p}{E} \frac{dN}{dy} \simeq J(\eta, \langle m \rangle / \langle p_T \rangle) \frac{dN}{dy}$$

GW, J.Phys. G40, 045104 (2013)

D. Roehrscheid, GW, Phys. Rev. C86, 024902 (2012)

$$J(\eta, \langle m \rangle / \langle p_T \rangle) = \cosh(\eta) \cdot$$

$$[1 + (\langle m \rangle / \langle p_T \rangle)^2 + \sinh^2(\eta)]^{-1/2}.$$

with the rapidity distribution in the three-sources model

$$\frac{dN_{ch}(y, t = \tau_{int})}{dy} = N_{ch}^1 R_1(y, \tau_{int}) + N_{ch}^2 R_2(y, \tau_{int}) + N_{ch}^{eq} R_{eq}(y, \tau_{int}).$$

and the rapidity

$$y = 0.5 \cdot \ln((E + p)/(E - p))$$

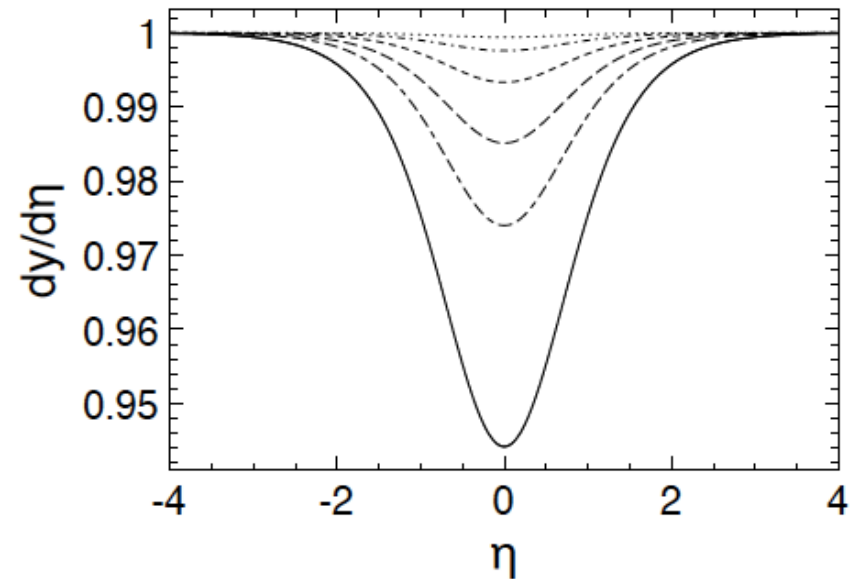
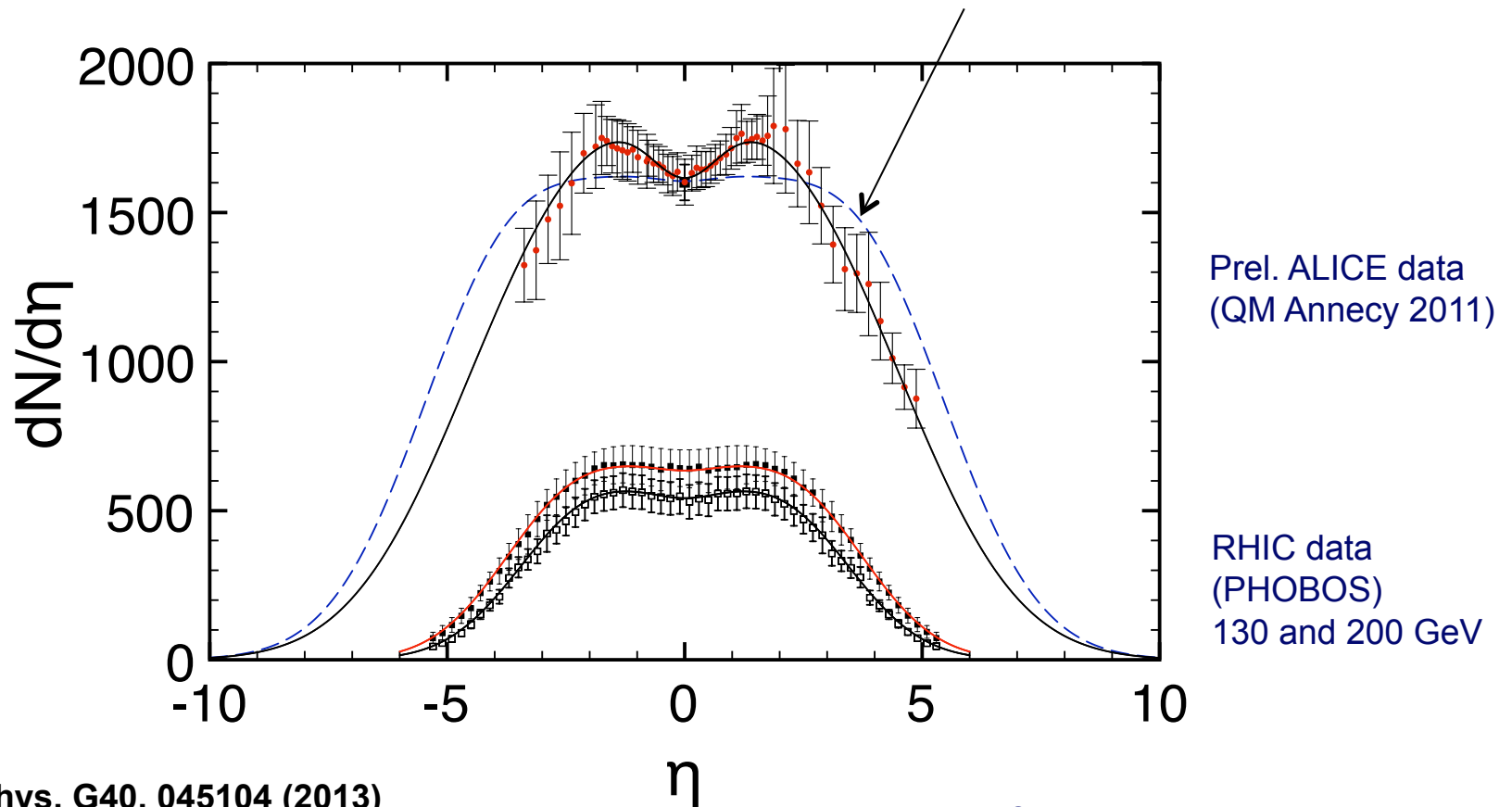


Figure 1: The Jacobian  $dy/d\eta$  for  $\langle m \rangle = m_\pi$  and average transverse momenta (bottom to top)  $\langle p_T \rangle = 0.4, 0.6, 0.8, 1.2, 2$  and  $4$  GeV/c.

# Comparing data with the RDM prediction for produced charged hadrons

Central PbPb @ 2.76 TeV

Prediction GW in PLB 698, 411 (2011)



GW, J. Phys. G40, 045104 (2013)

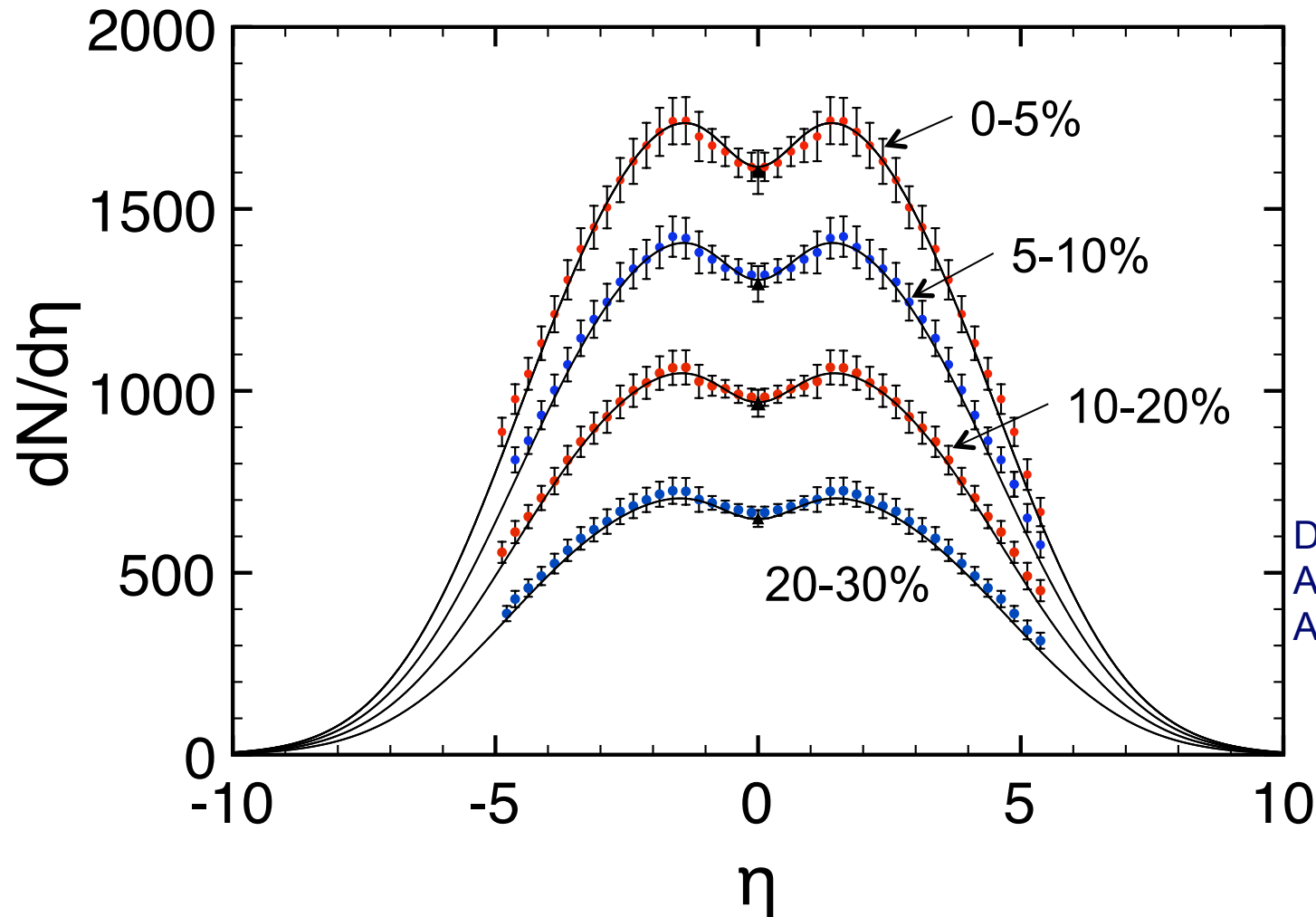
$$dN/d\eta (\eta \approx 0) = 1584 \pm 4 \text{ (stat.)} \pm 76 \text{ (sys.)} \quad [1]$$

$$1601 \pm 60 \quad [2]$$

- [1] ALICE collab., PRL 105, 252301 (2010)
- [2] ALICE collab., PRL 106, 032301 (2011)
- [3] B.B. Back et al., PHOBOS coll., PRL 87, 102303 (2001); PRL 91, 052303 (2003); PRC 83, 024913 (2011)

# RDM $\chi^2$ fits to LHC/ALICE results for 2.76 TeV PbPb

GW, J. Phys. G40, 045104 (2013)



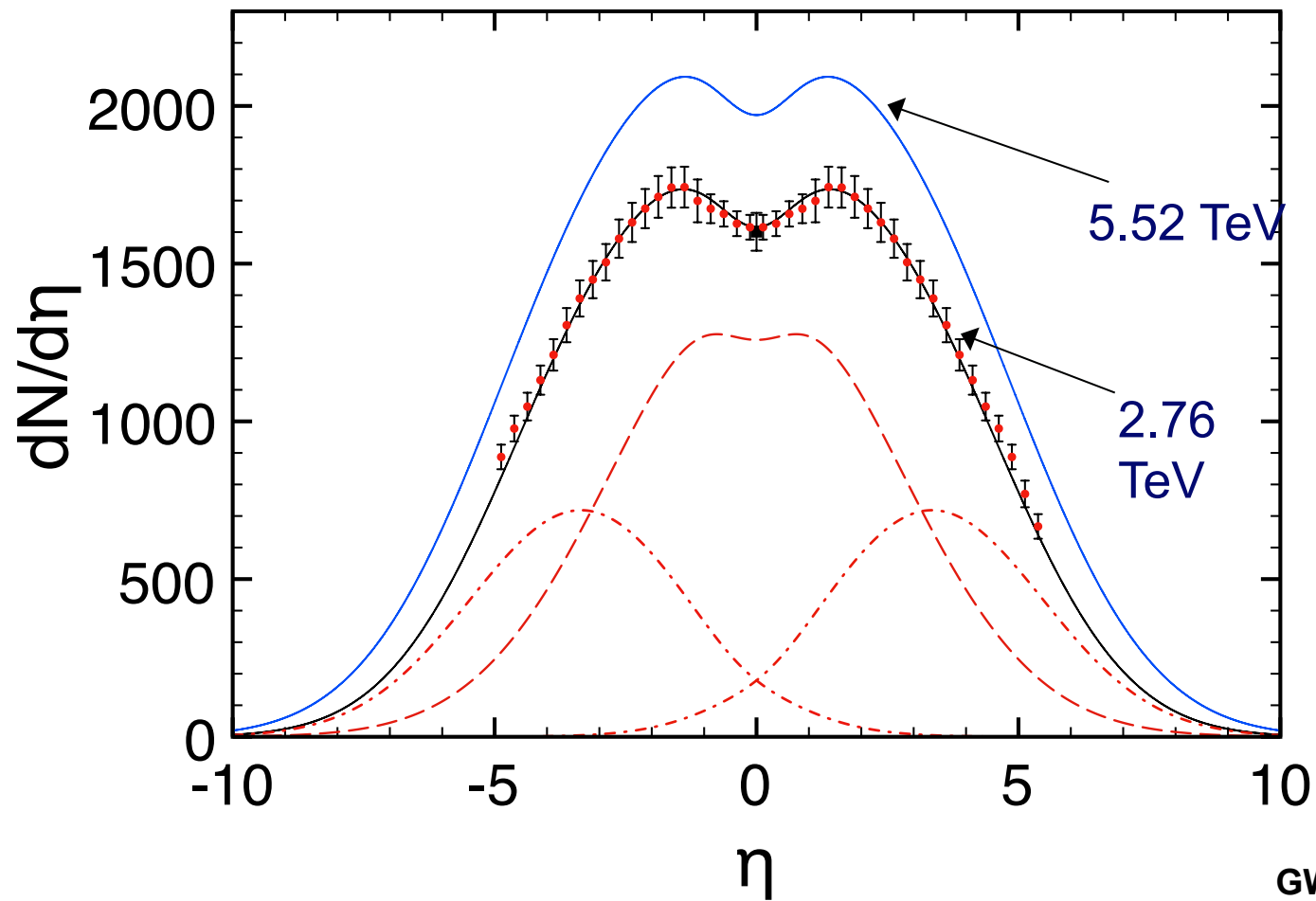
Data: M. Guilbaud et al.,  
ALICE Coll., Nucl. Phys.  
A 904-905, 381c (2013)

# Parameters of the 3-sources RDM at RHIC and LHC energies

**Table 1.** Three-sources RDM-parameters  $\tau_{int}/\tau_y$ ,  $\Gamma_{1,2}$ ,  $\Gamma_{gg}$ , and  $N_{gg}$ .  $N_{ch}^{1+2}$  is the total charged-particle number in the fragmentation sources,  $N_{gg}$  the number of charged particles produced in the central source. Results for  $\langle y_{1,2} \rangle$  are calculated from  $y_{beam}$  and  $\tau_{int}/\tau_y$ . Values are shown for 0–5% PbPb at LHC energies of 2.76 and 5.52 TeV in the lower two lines, with results at 2.76 TeV from a  $\chi^2$ -minimization with respect to the preliminary ALICE data [2], and using limited fragmentation as constraint. Corresponding parameters for 0–6% AuAu at RHIC energies are given for comparison in the upper four lines based on PHOBOS results [1]. Parameters at 5.52 TeV denoted by \* are extrapolated. Experimental midrapidity values (last column) are from PHOBOS [1] for  $|\eta| < 1$ , 0–6% at RHIC energies and from ALICE [13] for  $|\eta| < 0.5$ , 0–5% at 2.76 TeV.

$\sqrt{s_{NN}}$ (TeV)	$y_{beam}$	$\tau_{int}/\tau_y$	$\langle y_{1,2} \rangle$	$\Gamma_{1,2}$	$\Gamma_{gg}$	$N_{ch}^{1+2}$	$N_{gg}$	$\frac{dN}{d\eta} _{\eta \simeq 0}$
0.019	$\mp 3.04$	0.97	$\mp 1.16$	2.83	0	1704	-	$314 \pm 23$ [1]
0.062	$\mp 4.20$	0.89	$\mp 1.72$	3.24	2.05	2793	210	$463 \pm 34$ [1]
0.13	$\mp 4.93$	0.89	$\mp 2.02$	3.43	2.46	3826	572	$579 \pm 23$ [1]
0.20	$\mp 5.36$	0.82	$\mp 2.40$	3.48	3.28	3933	1382	$655 \pm 49$ [1]
2.76	$\mp 7.99$	0.87	$\mp 3.34$	4.99	6.24	7624	9703	$1601 \pm 60$ [13]
5.52	$\mp 8.68$	0.85*	$\mp 3.70$	5.16*	7.21*	8889*	13903*	1940*

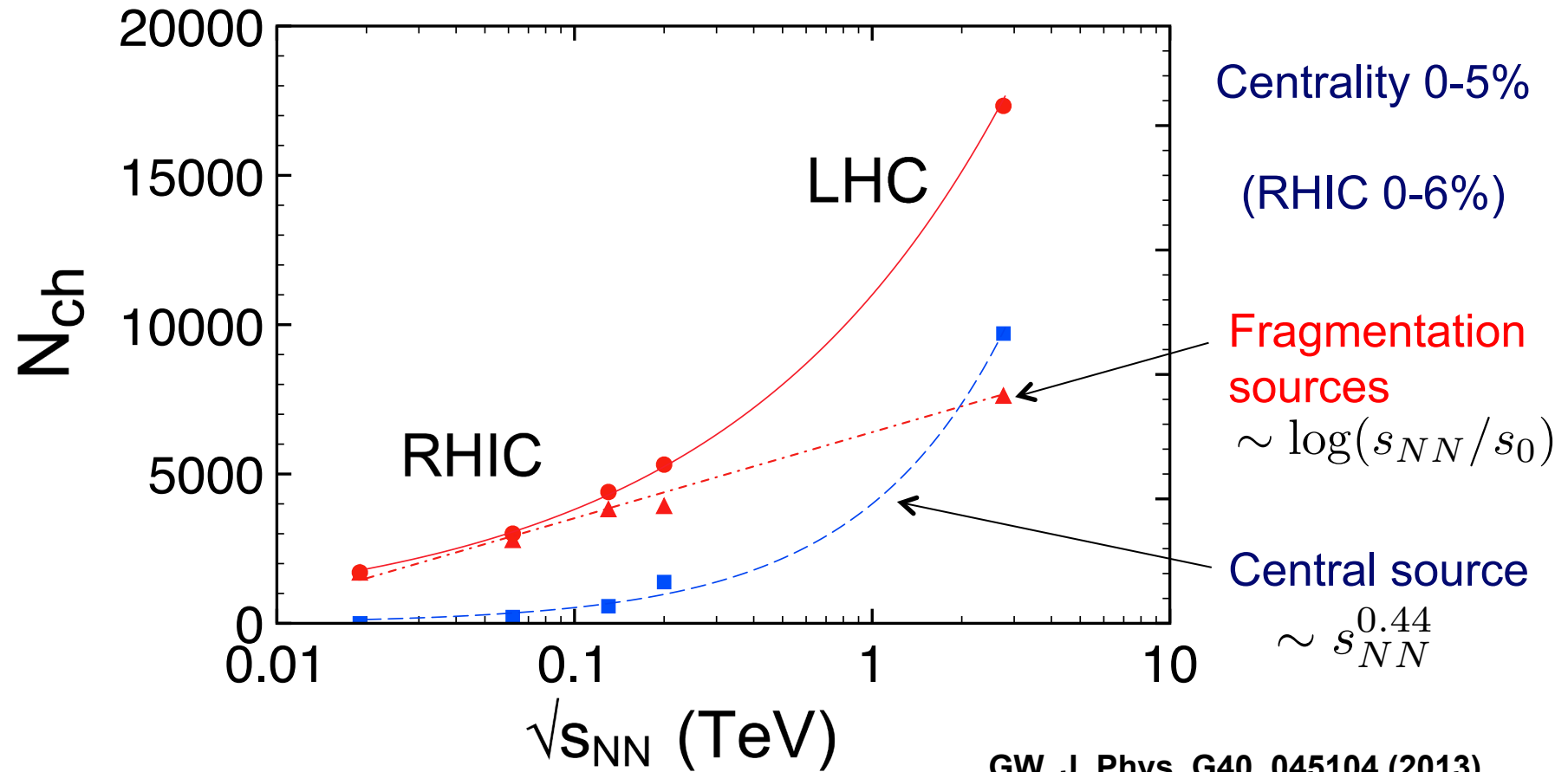
# 3 sources, and prediction for 5.52 TeV PbPb



Centrality 0-5%

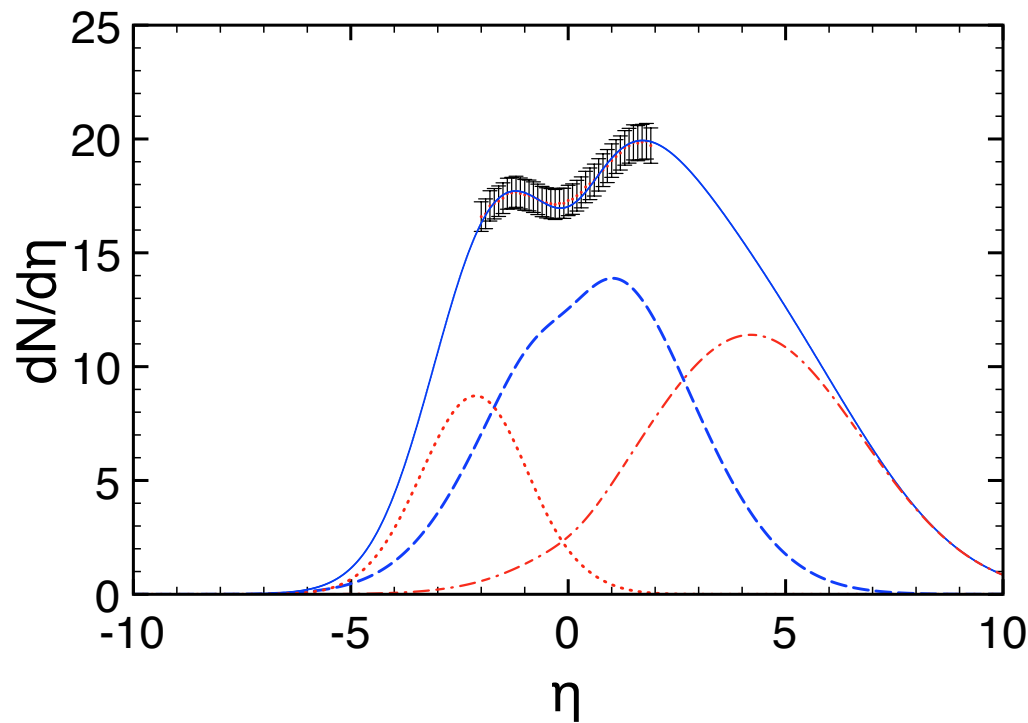
GW, J. Phys. G40, 045104 (2013)

# Content of the sources as function of energy



# 3-sources model (RDM): pPb @ 5.02 TeV

Min. bias 5.02 TeV pPb @ LHC



$$p_p = 4 \text{ TeV}/c$$

$$\sqrt{s_{NN}} = \sqrt{\frac{Z_1 * Z_2}{(A_1 * A_2)}} * 2p_p = 5.02 \text{ TeV}$$

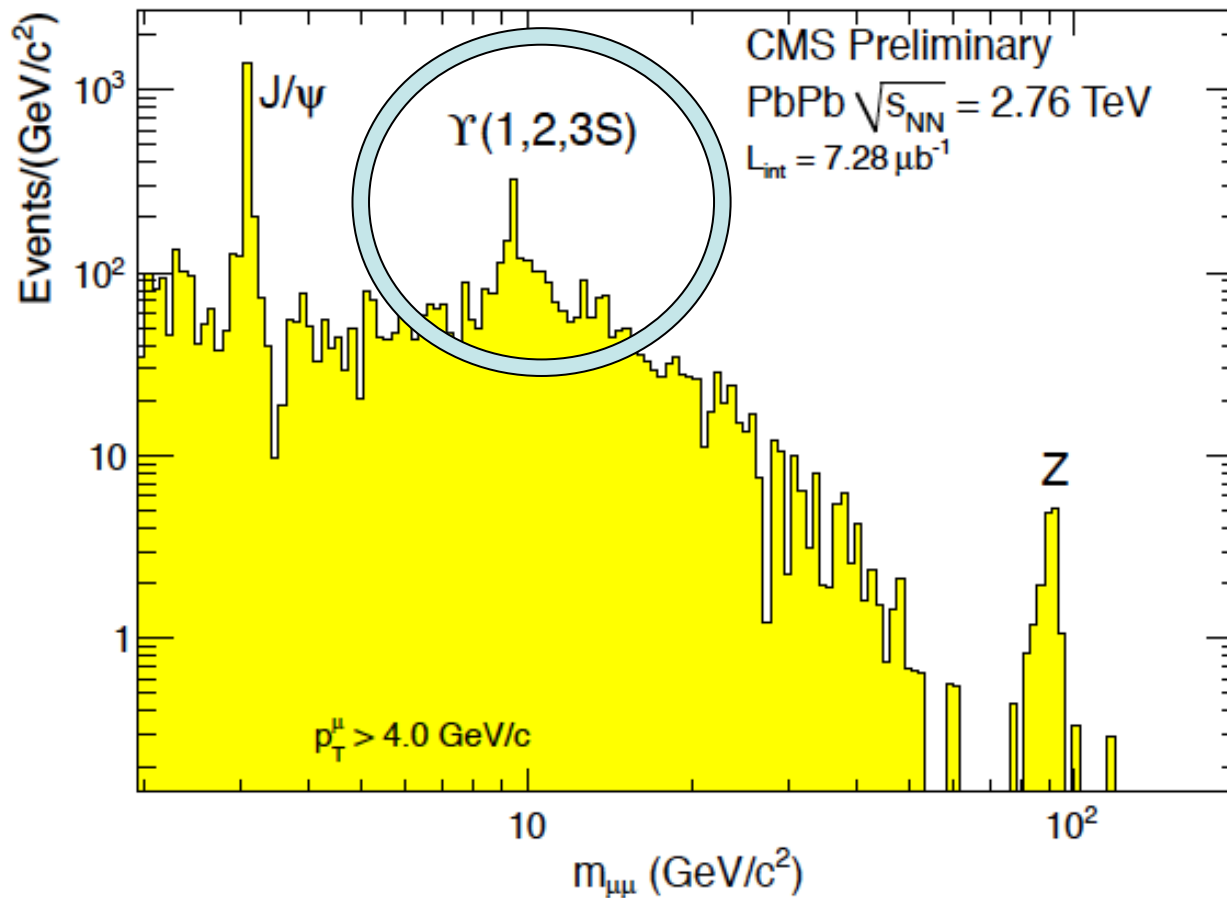
$$y_{\text{beam}}^{cm} = \mp \ln(\sqrt{s_{NN}}/m_0) \\ = \mp 8.586$$

Calculation: GW, J. Phys. G40, 045104 (2013)  
Midrap. data: ALICE collab., PRL 110, 032301 (2013)

# Conclusion Particle production

- ❖ Charged-hadron production at RHIC and LHC energies has been described in a Relativistic Diffusion Model (RDM).
- ❖ Predictions of pseudorapidity distributions  $dN/d\eta$  of produced charged hadrons in the 3-sources RDM at LHC energies rely on the extrapolation of the diffusion-model parameters with  $\ln(\sqrt{s_{NN}})$
- ❖ In agreement with a QCD-based microscopic model, the contribution of the fragmentation sources from quark-gluon collisions at LHC energies is very small at midrapidity, but substantial at larger values of pseudorapidity  $\eta$ .
- ❖ Between RHIC and LHC energies, the midrapidity gluon-gluon source becomes more important than the fragmentation sources.
- ❖ The centrality dependence of the three sources has been investigated in direct comparison with the preliminary ALICE data.

### 3. Upsilon Suppression in PbPb @ LHC



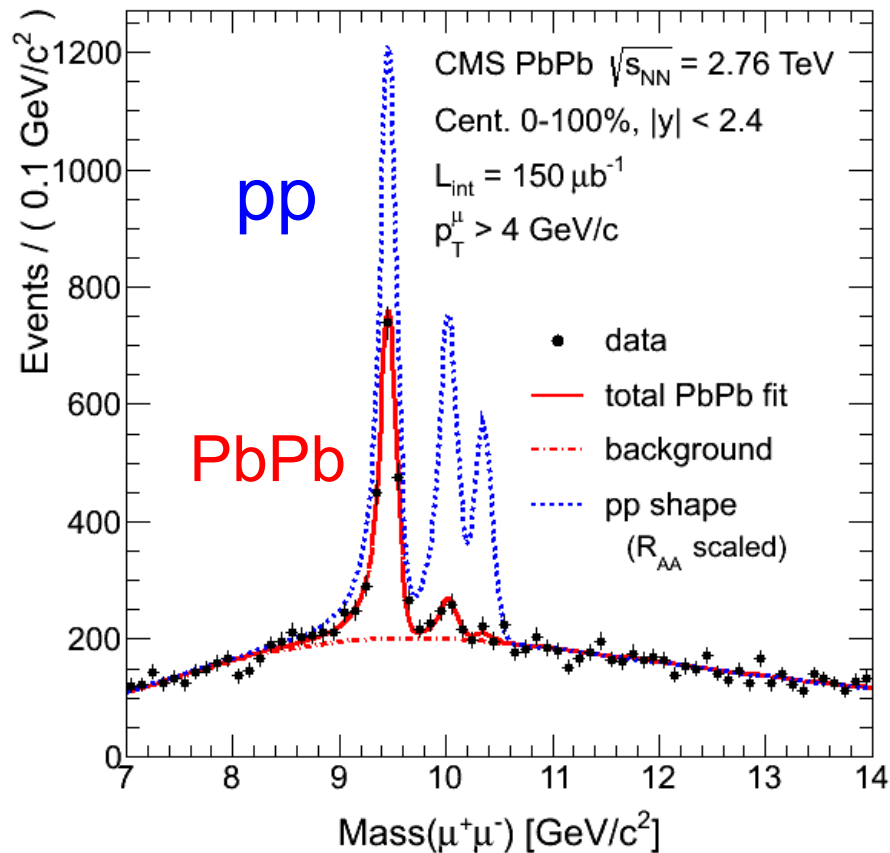
$\Upsilon$  suppression as a sensitive probe for the QGP

- No significant effect of regeneration
- $m_b \approx 3m_c$   $\Rightarrow$  cleaner theoretical treatment
- More stable than  $J/\psi$

$$E_B(Y_{1S}) \approx 1.10 \text{ GeV}$$
$$E_B(J/\psi) \approx 0.64 \text{ GeV}$$

# Y(nS) states are suppressed in PbPb @ LHC:

CMS



## A clear QGP indicator

1. Y(1S) ground state is suppressed in PbPb:

$$R_{AA}(Y(1S)) = 0.56 \pm 0.08 \pm 0.07 \text{ in min. bias}$$

2. Y(2S, 3S) states are > 4 times stronger suppressed in PbPb than Y(1S)

$$R_{AA}(Y(2S)) = 0.12 \pm 0.04 \text{ (stat.)} \pm 0.02 \text{ (syst.)}$$

$$R_{AA}(Y(3S)) = 0.03 \pm 0.04 \text{ (stat.)} \pm 0.01 \text{ (syst.)}$$

$$R_{AA} = \frac{N_{PbPb}(Q\bar{Q})}{N_{coll}N_{pp}(Q\bar{Q})}$$

CMS Collab., PRL 109, 222301 (2012)  
[Plot from CMS database]

# Screening, Gluodissociation and Collisional broadening of the $Y(nS)$ states

- Debye screening of all states involved: **Static suppression**
- The **imaginary part** of the potential (effect of collisions) contributes to the broadening of the  $Y(nS)$  states: **damping**
- **Gluon-induced dissociation**: **dynamic suppression**, in particular of the  $Y(1S)$  ground state due to the large thermal gluon density
- **Feed-down** from the excited  $Y$  states to the ground state substantially modifies the populations: **indirect suppression**

F. Vaccaro, F. Nendzig and GW, Europhys.Lett. 102, 42001 (2013)

F. Nendzig and GW, Phys. Rev. C 87, 024911 (2013)

F. Brezinski and GW, Phys. Lett.B 70, 534 (2012)

## Screening and damping treated in a nonrelativistic potential model

$$V(r, T) = \sigma r_D \left[ 1 - e^{-r/r_D} \right] - \frac{4\alpha_s^s}{3} \left[ \frac{1}{r_D} + \frac{1}{r} e^{-r/r_D} \right] \\ - i \frac{4\alpha_s^s}{3} T \int_0^\infty dz \frac{2z}{(1+z^2)^2} \left[ 1 - \frac{\sin(rz/r_D)}{(rz/r_D)} \right]$$

Screened potential:  $r_D$  Debye radius,  $\alpha_s^s \geq 0.4$  the strong coupling constant at the soft scale  $\alpha_s^s = \alpha_s(\langle 1/r \rangle(T, E, \Gamma))$  accounting for short-range Coulomb exchange,  $\sigma \approx 0.192$  the string tension (Jacobs et al.; Karsch et al.)

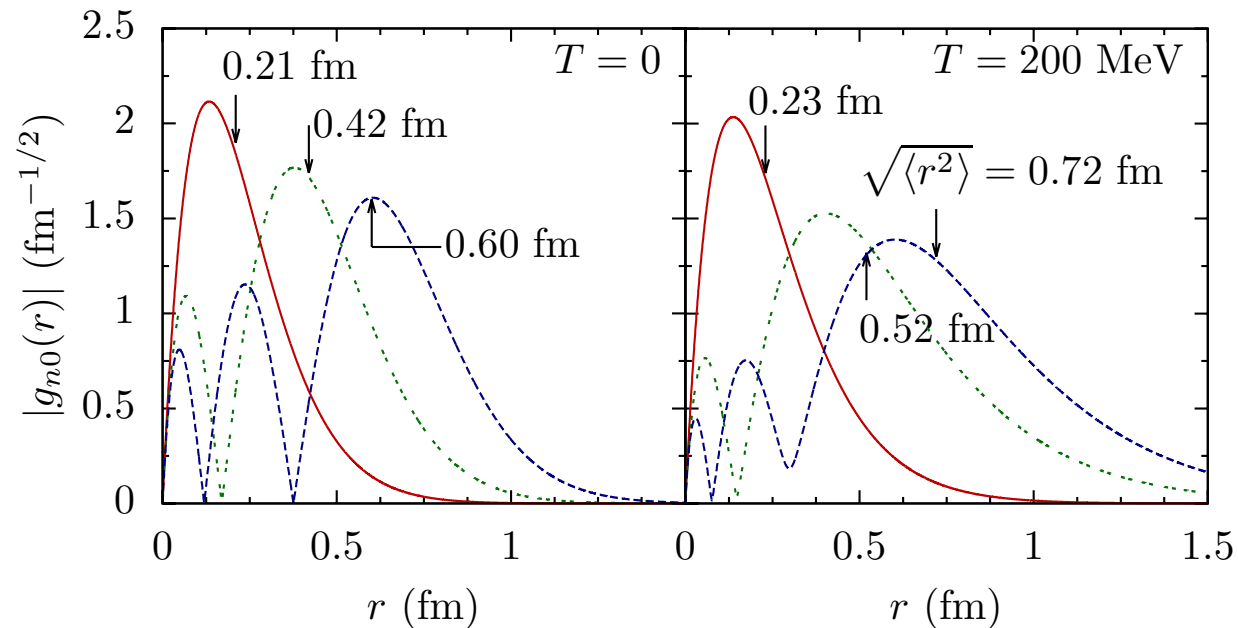
Imaginary part: Collisional damping (Laine et al. 2007, Beraudo et al. 2008, Brambilla et al. 2008) for  $2\pi T \gg \langle 1/r \rangle$ ; different form for  $2\pi T \ll \langle 1/r \rangle$ .

$$r_D^{-1} = T \left[ 4\pi\alpha_s(2N_c + N_f)/6 \right]^{1/2} = m_D, \text{ Debye mass}$$

# Radial wave functions of $Y(nS)$ states

Starting from the Schrödinger equation with complex potential  $V(r,T)$  for the wave functions  $\psi(r,T)$ ,  
the numerical solution of the radial equation

$$[H(r, T, \alpha_s) - E + i\Gamma/2]g(r) = 0 \quad \text{becomes}$$



Radial wave functions (abs. values) of  $Y(1S, 2S, 3S)$  – red, green, blue – for  $T = 0$  (left) and  $T = 200$  MeV (right). The  $Y(1S)$  groundstate is very stable against screening for  $T < 4.1 T_C$

From: F. Nendzig and G. Wolschin

# Cross section for gluodissociation

Born amplitude for the interaction of gluon clusters according to Bhanot&Peskin in dipole approximation / Operator product expansion, extended to include the screened coulombic + string eigenfunctions as outlined in Brezinski and Wolschin, PLB 70, 534 (2012)

$$\sigma_{diss}^{nS}(E) = \frac{2\pi^2 \alpha_s E}{9} \int_0^\infty dk \delta\left(\frac{k^2}{m_b} + \epsilon_n - E\right) |w^{nS}(k)|^2$$
$$w^{nS}(k) = \int_0^\infty dr r g_{n0}^s(r) g_{k1}^a(r)$$

for the Gluodissociation cross section of the  $Y(nS)$  states, and correspondingly for the  $\chi_b(nP)$  states.

# Gludissociation cross section

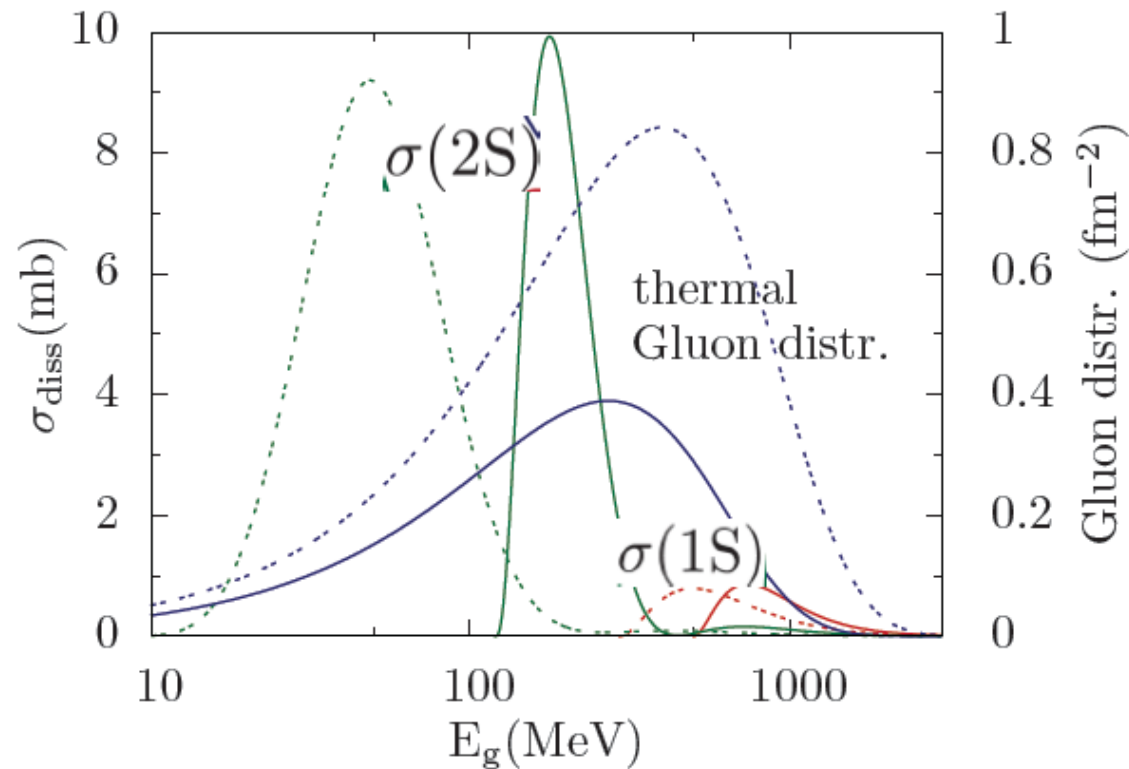


Figure 2: (color online) Gluodissociation cross sections  $\sigma_{diss}(nS)$  in mb (lhs scale) of the  $\Upsilon(1S)$  and  $\Upsilon(2S)$  states calculated using the screened wave functions calculated from the complex potential eq. (1) for temperatures  $T = 170$  (solid curves) and 250 MeV (dotted curves) as functions of the gluon energy  $E_g$ . The thermal gluon distribution (rhs scale, solid curve for  $T = 170$  MeV, dotted for 250 MeV) is used to obtain the thermally averaged gluodissociation cross sections.

F. Brezinski and GW, PLB 707 (2012) 534 /

F. Nendzig and GW, Nucl. Phys. A 910-911 (2013) 458

# Dynamical fireball evolution

Dependence of the local temperature  $T$  on impact parameter  $b$ , time  $t$ , and transverse coordinates  $x, y$  (Bjorken scaling for the time evolution):

$$T(b, t, x, y) = T_c \frac{T_{AA}(b, x, y)}{T_{AA}(0, 0, 0)} \left( \frac{t_{\text{QGP}}}{t} \right)^{1/3}$$

with the nuclear overlap (thickness function)  $T_{AA}(b, x, y)$ .

The number of produced  $b\bar{b}$ -pairs is proportional to the number of binary collision, and the nuclear overlap

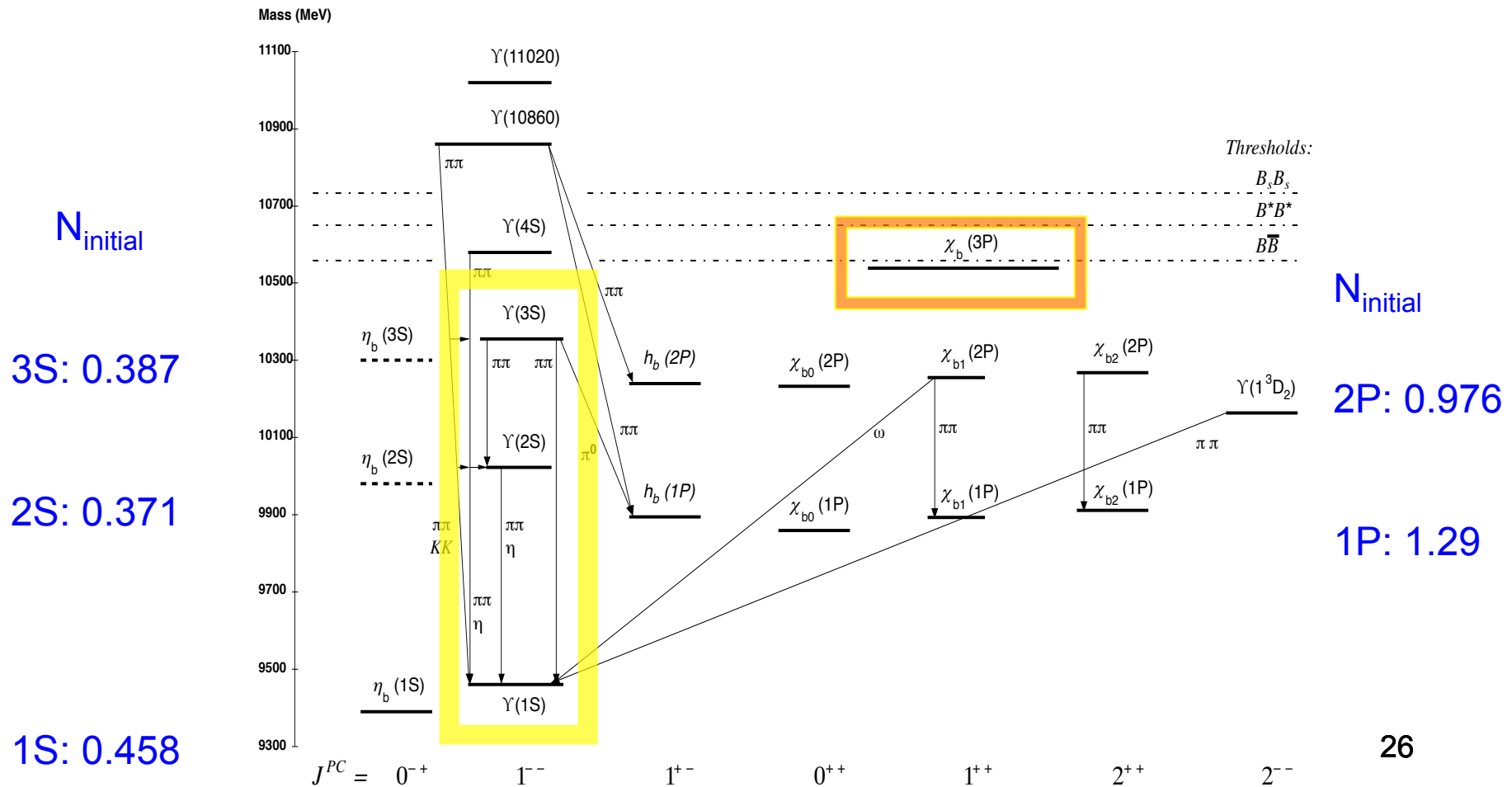
$$N_{b\bar{b}}(b, x, y) \propto N_{\text{coll}}(b, x, y) \propto T_{AA}(b, x, y)$$

Preliminary suppression factor (without feed-down):

$$R_{AA}^{\text{prel}} = \frac{\int d^2b \int dx dy T_{AA}(b, x, y) e^{-\int_{t_F}^{\infty} dt \Gamma_{\text{tot}}(b, t, x, y)}}{\int d^2b \int dx dy T_{AA}(b, x, y)}$$

# Feed-down cascade including $\chi_{nP}$ states

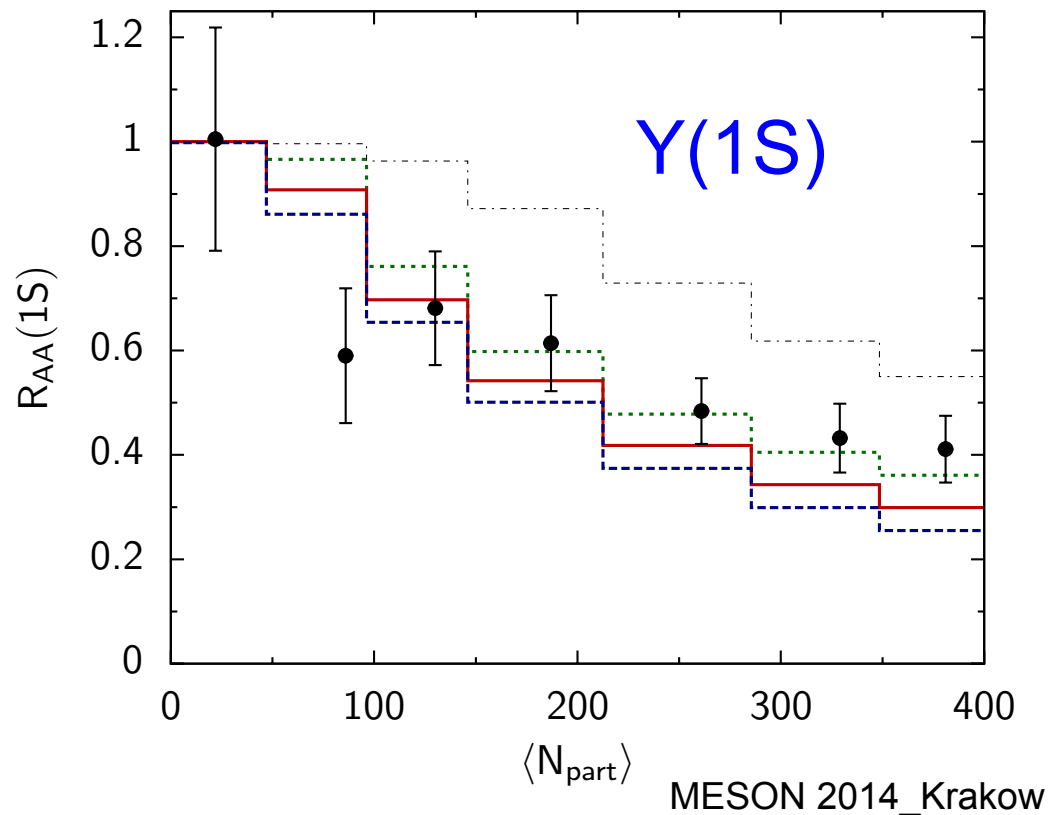
Relative initial populations in pp computed using an inverted cascade from the final populations measured by CMS and CDF ( $\chi_b$ )  
 $[N_{\text{final}}(1S):=1]$



# Theoretical vs. exp. (CMS) Suppression factors

- Screening (potential model)
- Gluodissociation (OPE with string tension included)
- Collisional damping (imaginary part of potential)
- Feed-down from excited states

$t_F$ : Y formation time  
 $t_{QGP}$ : QGP lifetime  
 $T_{max}$  @  $t_F$ : 200-800 MeV



$t_F = 0.1$  fm/c  
 $t_{QGP} = 4, 6, 8$  fm/c

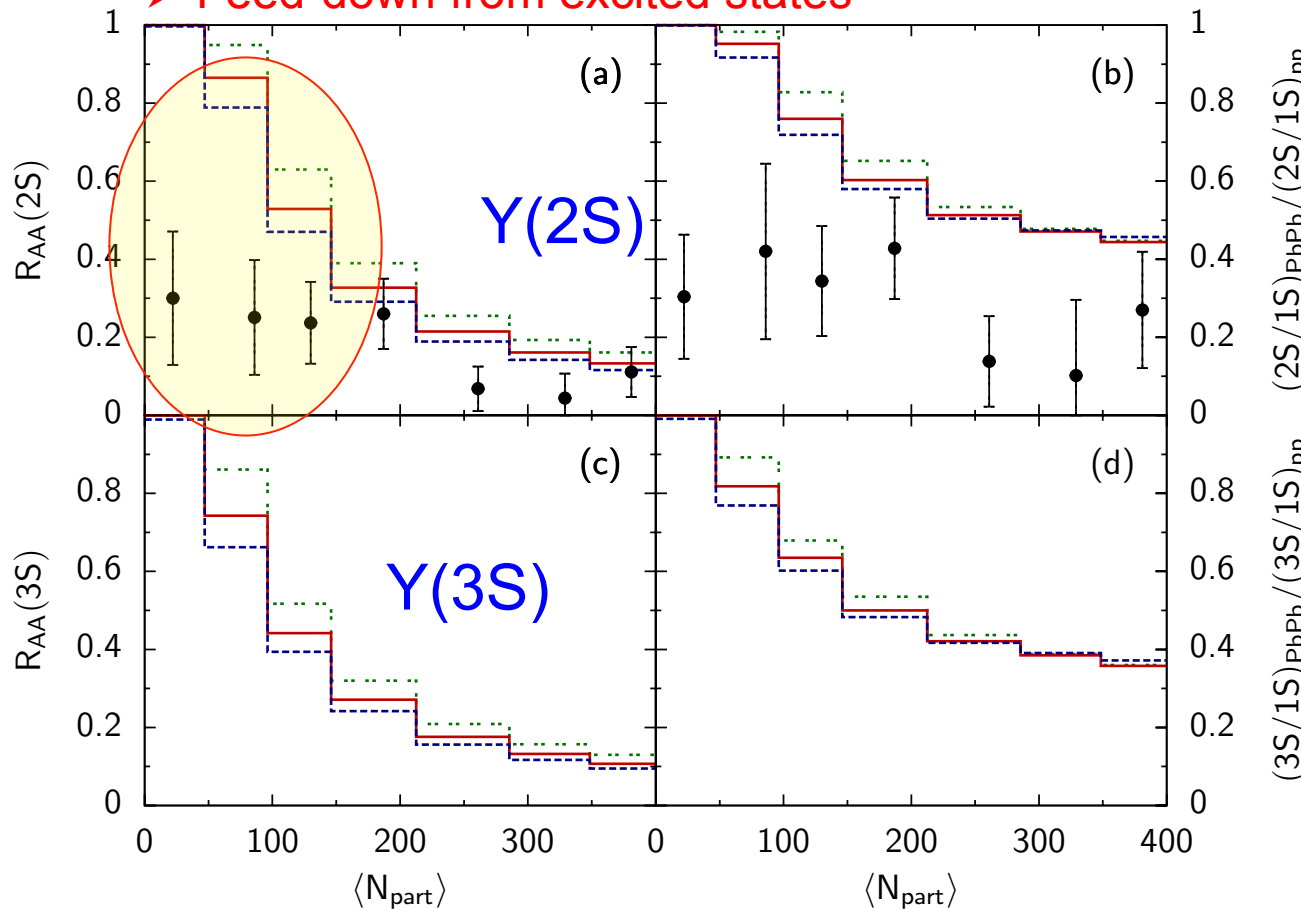
# Theoretical vs. exp. (CMS) Suppression factors

- Screening (potential model)
- Gluodissociation (OPE with string tension included)
- Collisional damping (imaginary part of potential)
- Feed-down from excited states

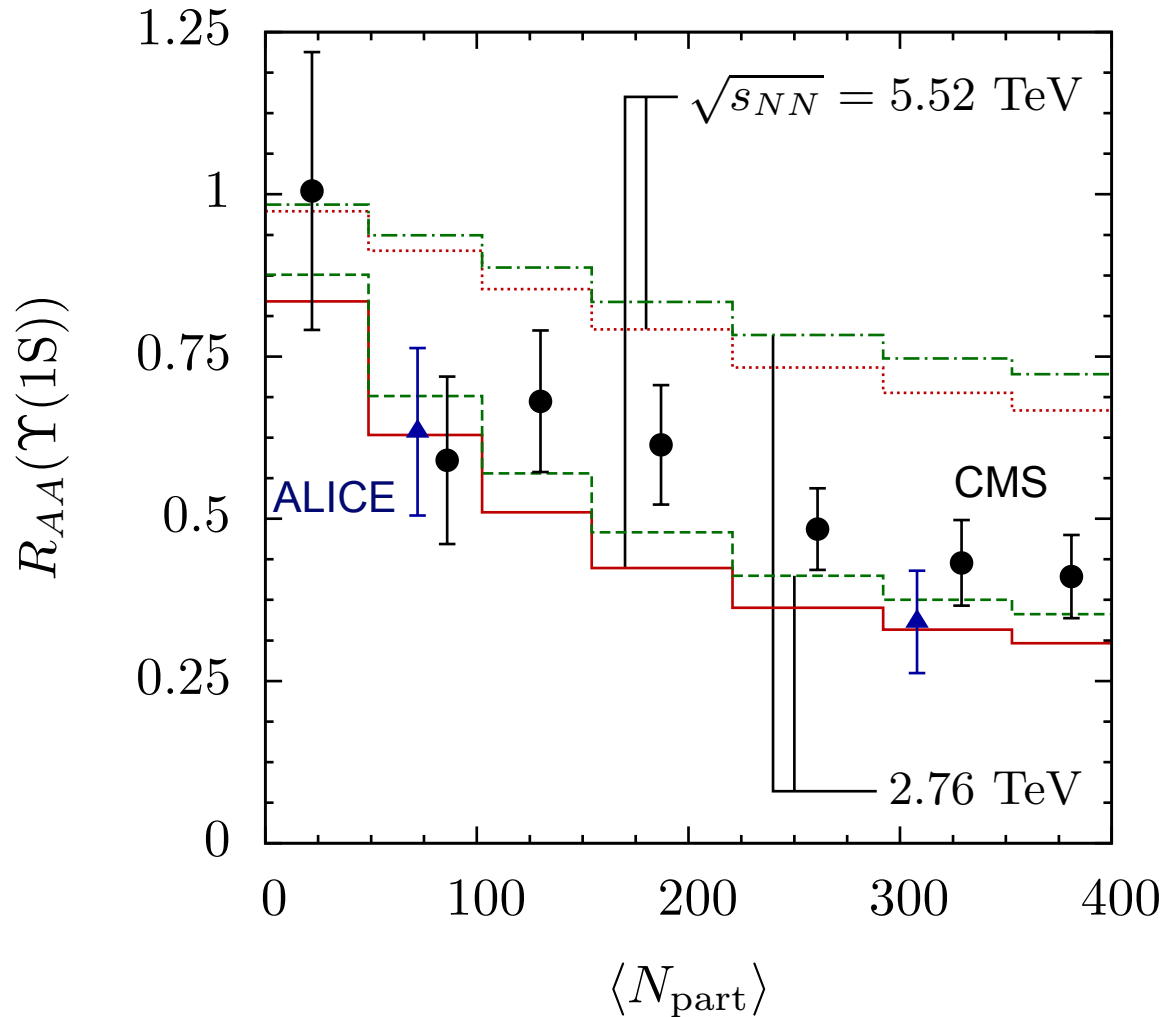
$t_F$ : Y formation time  
 $t_{QGP}$ : QGP lifetime  
 $T_{max}$  @  $t_F$ : 200-800 MeV

$t_F = 0.1$  fm/c  
 $t_{QGP} = 4, 6, 8$  fm/c

Leaves room for additional suppression mechanisms for the excited states:  
**Hadronic dissociation**, mostly by pions, is one possibility



# Prediction for $\Upsilon(1S)$ suppression at 5.52 TeV



Use scaling relation between initial entropy density and charged particle multiplicity

$$s_0 \propto dN_{ch}/d\eta \propto T_0^3$$

Yields initial temperature increase of 6.6 % at 5.5 TeV, and less than 10% more suppression.

# Conclusion Upsilon suppression

- ❖ The suppression of the  $\Upsilon(1S)$  ground state in PbPb collisions at LHC energies through gluodissociation, damping, reduced feed-down and screening has been calculated for min. bias, and as function of centrality, and is found to be in good agreement with the CMS result. Screening is not decisive for the 1S state except for central collisions.
- ❖ The enhanced suppression of the  $\Upsilon(2S, 3S)$  relative to the 1S state in PbPb as compared to pp collisions at LHC energies (CMS) is consistent with the model within the (large) error bars for central collisions. There is room for additional suppression mechanisms, in particular for peripheral collisions where discrepancies to the CMS data persist. Hadronic dissociation of the excited states may be relevant.

Thank you for your attention,

and for organizing MESON 2014 !